Inorganic Chemistry

Article

pubs.acs.org/IC

A Modulated Hydrothermal (MHT) Approach for the Facile Synthesis of UiO-66-Type MOFs

Zhigang Hu, Yongwu Peng, Zixi Kang, Yuhong Qian, and Dan Zhao*

Department of Chemical & Biomolecular Engineering, National University of Singapore, 4 Engineering Drive 4, 117585, Singapore

Supporting Information

ABSTRACT: Developing a general and economically viable approach for the large-scale synthesis of water-stable metal−organic frameworks (MOFs) with repeatable quality remains the key step for their massive production and commercialization. We herein report a green (aqueous solutions), mild (100 °C, 1 atm), and scalable (can be up to kilograms) modulated hydrothermal (MHT) synthesis of UiO-66, an iconic MOF that has been widely studied recently for its high water stability. More importantly, the MHT synthetic approach can be applied to synthesize other water-stable MOFs with structures identical to UiO-66, such as UiO-66-$(F)_4$, UiO-66-$(OCH_2CH_3)_2$, and UiO-66-$(COOH)_4$, which cannot be obtained via the traditional solvothermal method. Their performance in postcombustion CO_2 capture has also been evaluated. Our MHT approach has clearly depicted a roadmap for the facile synthesis of zirconium-based water stable MOFs to facilitate their massive production and commercialization.

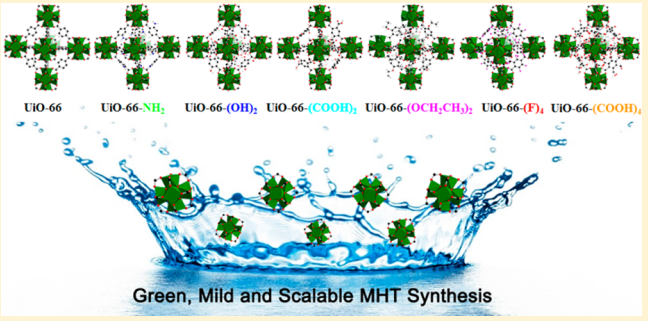

INTRODUCTION

Metal−organic frameworks (MOFs), also known as porous coordination polymers (PCPs), are emerging porous crystalline materials composed of inorganic metal nodes and organic linkers.[1,2] The last two decades have witnessed ample studies of MOFs and their applications in gas storage and separation, chemical sensing, functional catalysis, etc., owing to their ultrahigh porosities, tunable pore size and structures, and plentiful chemical functionalities.[3,4] However, most of the reported MOFs so far suffer from their weak hydrothermal stabilities that prevent their industrial applications.[5] Although several MOFs of prominent hydrothermal stabilities have been reported, such as MILs,[6] ZIFs,[7] pyrazolate-bridged MOFs,[8] Zr and Hf based MOFs (especially UiO-66),[9−17] F-containing MOFs,[18] etc., their repeatable synthesis and scale-up still remain as a big challenge for their mass production. For example, most MOFs are synthesized by the so-called solvothermal method,[19] which requires high temperature and pressure, expensive organic solvents, and sophisticated separation procedures that can dramatically increase the cost and make it hard for scale-up production. It is therefore of paramount importance to develop facile synthetic approaches for MOFs, especially those water-stable ones with high commercial value. Several trials have been reported. For example, the mechanochemical synthesis has been proved to be quite efficient, but is mainly for ZIFs so far.[20] Flow reactors have been used for a continuous synthesis of several well-known MOFs, such as HKUST-1, MOF-5, UiO-66, etc., while the throughput remains to be studied.[21,22] Recently, a simple water-reflux synthetic method was adopted to synthesize a new UiO-66-type MOF UiO-66-$(COOH)_2$ in kilogram scale.[23] However, in our attempts to repeat this work we always ended up with hard-rock-like products with poor processability and repeatability. In addition, the crystallinity of the product was still far from satisfactory.[24]

We herein report a general modulated hydrothermal (MHT) approach to synthesize a series of UiO-66-type MOFs with repeatable quality and ability to be easily scaled up (Scheme 1). This method can be applied not only for the synthesis of reported UiO-66-type MOFs, such as UiO-66, UiO-66-NH_2, UiO-66-$(OH)_2$, and UiO-66-$(COOH)_2$, but also for several new MOFs such as UiO-66-$(F)_4$, UiO-66-$(OCH_2H_3)_2$, and UiO-66-$(COOH)_4$. Our approach has delineated an explicit blueprint to the scale-up synthesis of the promising UiO-66-type MOFs for their mass production and commercialization.

MATERIALS AND METHODS

Materials and Equipment. All of the reagents used were obtained from commercial suppliers and were used without further purification. NMR data were collected on a Bruker Avance 500 MHz NMR spectrometer (DRX500). Field-emission scanning electron microscope (FE-SEM) analyses were conducted on an FEI Quanta 600 SEM (20 kV) equipped with an energy dispersive spectrometer (EDS, Oxford Instruments, 80 mm^2 detector). Samples were treated via Pt sputtering before observation. Powder X-ray diffraction patterns were obtained on a Bruker D8 Advance X-ray powder diffractometer equipped with a Cu sealed tube (λ = 1.54178 Å) at a scan rate of 0.02 deg s^{-1}. TGA

Received: February 23, 2015
Published: May 1, 2015

DOI: 10.1021/acs.inorgchem.5b00435
Inorg. Chem. 2015, 54, 4862−4868

Scheme 1. (a) BDC-Type Ligands Used in This Study[a] and (b) MHT Synthesis of UiO-66-Type MOFs

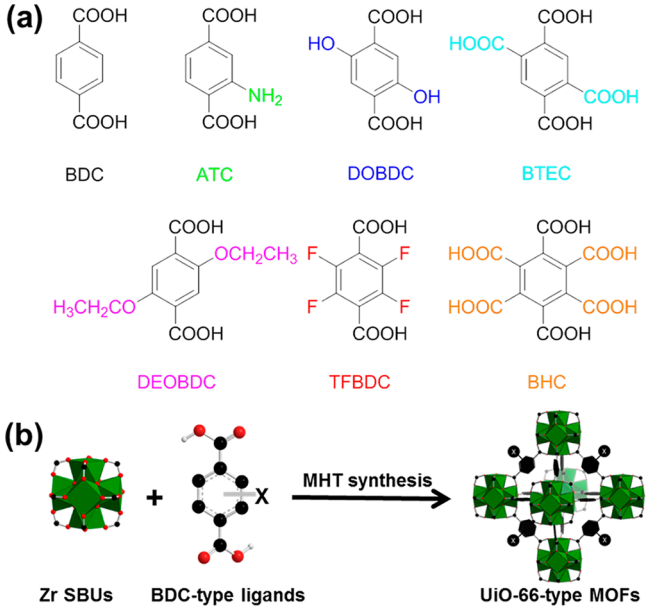

[a]BDC: benzene-1,4-dicarboxylic acid.

were performed using a Shimadzu DTG-60AH thermal analyzer under flowing N_2 gas (100 mL min^{-1}) with a heating rate of 10 °C min^{-1}.

Synthesis of 2, 5-Diethyloxyterephthalic Acid (DEOBDC). 2,5-Dihydroxyterephthalic acid (1.0 g, 5 mmol) and potassium carbonate (4 g) were suspended in 40 mL of *N*,*N*-dimethylformamide (DMF). Bromoethane (EtBr, 1.5 mL) was slowly added into the mixture, which was heated to 90 °C under stirring for 24 h. Upon cooling, the mixture was slowly poured into ice−water and stirred for another 30 min. The yielded suspension was filtered and washed with water several times to give a pale yellow solid. The crude solid was dissolved in a mixed solvent of THF/MeOH/H_2O (15 mL/15 mL/5 mL), followed by the addition of LiOH·H_2O (2.0 g) and was heated at 70 °C for 10 h. The solution was cooled to room temperature, then acidified to pH ∼2, and finally extracted with Et_2O/H_2O. The organic layer was collected and dried over $MgSO_4$ and evaporated under reduced pressure to give a white solid of 2,5-diethoxyterephthalic acid. Yield: 1.08 g (85%). ^{1}H NMR (400 MHz, DMSO-d_6) δ: 7.26 (s, 2H, ArH), 4.00−4.07 (q, 4H, CH_2), 1.24−1.31 (t, 6H, CH_3).

MHT Synthesis of UiO-66-Type MOFs. In a typical process, organic ligand (∼5 mmol) and $Zr(NO_3)_4$ (1.8 g, ∼5.2 mmol) were suspended in 50 mL of water/acetic acid mixed solvent with various ratios (Table S1 in the Supporting Information), and the reaction mixture was heated under reflux for 24 h to yield a powder product. The product was soaked in anhydrous methanol for 3 days at room temperature, during which time the extract was decanted and fresh methanol was added every day. Then the sample was treated with anhydrous dichloromethane similarly for another 3 days. This process was carried out to wash out residual reagents in the pores. After removal of dichloromethane by decanting, the sample was dried under a dynamic vacuum at 120 °C for 24 h to yield the final product with a yield of 63−95% based on the overall weight of ligand and metal salt.

Gas and Water Sorption Measurements. Gas and water sorption isotherms of UiO-66-type MOFs were measured up to 1 bar using a Micromeritics ASAP 2020 surface area and pore size analyzer. Before the measurements, the sample (∼80 mg) was degassed under reduced pressure (<10^{-2} Pa) at 150 °C for 10 h. UHP grade N_2 and CO_2 were used for gas sorption measurements. Oil-free vacuum pumps and oil-free pressure regulators were used to prevent contamination of the samples during the degassing process and isotherm measurement. The temperatures of 77, 273, and 298 K were maintained with a liquid nitrogen bath, with an ice water bath, and under room temperature, respectively. Pore size distribution data were calculated from the N_2 sorption isotherms at 77 K based on nonlocal density functional theory (NLDFT) model in the Micromeritics ASAP 2020 software package (assuming slit pore geometry).

RESULTS AND DISCUSSION

Structural Characterizations. It has been reported that acid modulators, such as trifluoroacetic acid, hydrochloride acid, formic acid, etc., can be used to improve the crystallinity of MOFs during solvothermal reactions.[25−29] Our MHT approach is based on the same principle of precise pH control of the reaction media. In our trials of optimizing the synthesis of UiO-66-$(COOH)_2$, we have found that adding 70 equiv (molar ratio) of acetic acid (AA) as a modulator into the aqueous reaction medium could dramatically improve the crystallinity of the solid product, which can be collected as free powder with a much better processability (Figure S1 in the Supporting Information). Inspired by this finding, we used the MHT approach to successfully synthesize several reported UiO-66-type MOFs including UiO-66, UiO-66-NH_2, and UiO-66-$(OH)_2$ (Table S1 in the Supporting Information). Besides reported MOFs, our MHT approach can be extended to the synthesis of new UiO-66-type MOFs as well. We have designed and synthesized a new ligand, 2,5-diethyloxy-1,4-benzenedicarboxylic acid (DEOBDC), which was used to prepare a new UiO-66-type MOF UiO-66-$(OCH_2CH_3)_2$ based on the MHT approach (Table S1 in the Supporting Information). 2,3,5,6-Tetrafluoro-1,4-benzenedicarboxylic acid (TFBDC) is a commercially available ligand which in principle can be used to construct a UiO-66-type MOF. However, the expected UiO-66-$(F)_4$ could not be synthesized via the traditional solvothermal approach based on our year-long experiments. When the MHT approach was applied, UiO-66-$(F)_4$ could be facilely obtained with excellent crystallinity confirming its UiO-66-type structure (Figure 1). An even distribution of F inside

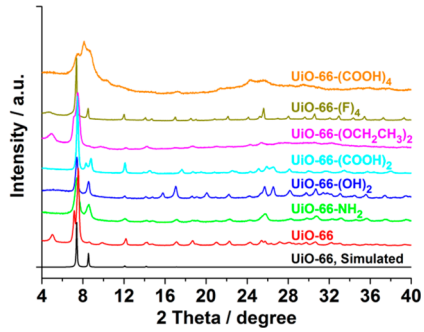

Figure 1. PXRD patterns of seven UiO-66-type MOFs synthesized through the MHT approach.

the MOF was also confirmed by EDS elemental mapping (Figure S2 in the Supporting Information). Another commercially available ligand we have tried is benzene-1,2,3,4,5,6-hexacarboxylic acid (BHC), which only gave clear solutions under solvothermal conditions but yielded solid precipitates named as UiO-66-$(COOH)_4$ when the MHT approach was applied.

The crystallinity and phase purity of MHT-synthesized UiO-66-type MOFs were evaluated by power X-ray diffraction (PXRD) (Figure 1). The simulated PXRD pattern of pristine UiO-66 is featured by two peaks at 7.4° and 8.5° representing the crystal plane (111) and (200), respectively. The PXRD

DOI: 10.1021/acs.inorgchem.5b00435
Inorg. Chem. 2015, 54, 4862−4868

patterns of most MHT-synthesized MOFs agree quite well with this pattern, indicating an isostructural UiO-66 framework topology. Although the crystallinity of UiO-66-$(COOH)_4$ remains to be improved, the broad peaks at ~8° still suggest a crystalline product with a framework topology identical to that of UiO-66. The unexpected peaks of ~5° in UiO-66, UiO-66-$(OCH_2CH_3)_2$, and UiO-66-$(F)_4$ suggest ordered crystal defects.[30−33] It has been reported that, by varying the synthetic conditions, ordered crystal defects can be generated within MOFs leading to extra PXRD peaks.[31] Considering that the ligands (BDC, DEOBDC, and TFBDC) in these three MOFs are more hydrophobic than the other four ligands (ATC, DOBDC, BTEC, and BHC), the ordered defects in these three MOFs could then possibly originate from the heterogeneity in the aqueous solutions in which BDC, DEOBDC, and TFBDC are insoluble even under reflux conditions while the other four ligands can be fully dissolved. It has been reported that defects in MOFs may generate extra exposed metal sites serving as Lewis acids that are helpful in gas storage/separation and heterogeneous catalysis.[34−37] Our MHT approach may bring the extra merit of denser Lewis acid sites to the synthesized MOFs which are beneficial in several applications.

The morphology of MOFs prepared in this study has been examined by field-emission scanning electron microscope (FE-SEM, Figure S3 in the Supporting Information). Unlike the solvothermally synthesized UiO-66 which has an octahedral crystal shape (Figure S3a in the Supporting Information), the MHT-synthesized samples exhibit various morphologies composed of tiny quasi-spherical particles with a size of 100−200 nm (Figure S3b−h in the Supporting Information). The small particle size may originate from the fast nucleation under water-reflux conditions in the presence of added modulators.[24] In addition, since the ligands adopted in this study have different polarities, they may have various molecular-level aggregations in aqueous solutions leading to different morphologies shown in Figure S3 in the Supporting Information. It was revealed by thermogravimetric analysis (TGA) that all the MHT-synthesized UiO-66-type MOFs exhibited high thermal stabilities up to 400 °C endowing their high-temperature applications (Figure 2).

BET Surface Area Analysis. N_2 sorption isotherms collected at 77 K were used to evaluate the surface area and porosity of the UiO-66-type MOFs. Almost all MOFs exhibit hybrid type I/IV isotherms with large hysteresis between adsorption and desorption branches (Figure 3a). Type I isotherms are indicative of microporous structure (pore size less than 2 nm) which is anticipated from the UiO-66 crystal model. Type IV isotherms are strong evidence of mesoporous structure (pore size lies between 2 and 50 nm) which may come from the interstitial voids between the nanoparticles of MHT-synthesized MOFs. Table 1 summarizes the surface area, porosity, and gas uptake properties of MOFs in this study. The Brunauer−Emmett−Teller (BET) surface area of UiO-66 synthesized herein is 769 $m^2\ g^{-1}$, which is lower than that of the sample prepared solvothermally (1580 $m^2\ g^{-1}$)[26] possibly due to the different degree of crystallinity under MHT conditions. However, it is interesting to note that our MHT approach has largely increased the surface area of several reported UiO-66-type MOFs. For example, the BET surface area of UiO-66-$(COOH)_2$ has been increased from the reported value of 415[23] to 494 $m^2\ g^{-1}$ in this study (~19% increase); the BET surface area of UiO-66-$(OH)_2$ has also increased (from 560[26] to 705 $m^2\ g^{-1}$, ~26% increase). The pore size distribution data reveal three major pores at 6, 9, and 12−13 Å in MHT-synthesized UiO-66, which agree quite well with the crystal model and reported values.[9] In the functionalized UiO-66 analogues such as UiO-66-NH_2, UiO-66-$(OH)_2$, UiO-66-$(OCH_2CH_3)_2$, etc., the pore size has been largely reduced because of the introduction of bulky groups (Figure 3b).[38]

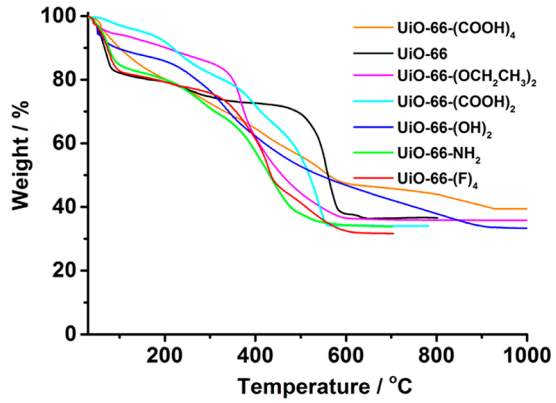

Figure 2. Thermogravimetric analysis (TGA) curves of UiO-66-type MOFs.

Gas Uptake and IAST CO_2/N_2 Selectivity. Adsorption-based postcombustion CO_2 capture has received tremendous attention recently.[39] The ideal adsorbents for this operation should have high working capacity (CO_2 uptake at 0.15 bar under ambient temperature such as 298 K), good CO_2/N_2 selectivity, excellent water stability, and low water interference.[40] MOFs have been demonstrated with great potential for this purpose.[40] The excellent water stability of MHT-synthesized MOFs reported herein prompts us to evaluate their performance in postcombustion CO_2 capture, which was done by analyzing the data of low pressure (up to 1 bar) CO_2 and N_2 sorption isotherms collected at both 273 and 298 K (Figure 4 and Table 1). Generally speaking, MOFs containing polar functional groups tend to have stronger interactions with CO_2 leading to higher working capacity and selectivity.[41] This trend is confirmed herein. For example, the best CO_2 working capacity belongs to UiO-66-$(OH)_2$ (0.651 mmol g^{-1}), which is 76% higher than that of the pristine UiO-66 (0.37 mmol g^{-1}).[38] Synthesized through our optimized MHT approach, UiO-66-$(COOH)_2$ has a CO_2 working capacity of 0.62 mmol g^{-1} that is 195% higher than the previously reported value (0.21 mmol g^{-1}).[24] The low working capacity of UiO-66-$(COOH)_4$ (0.209 mmol g^{-1}) is probably due to its limited surface area. It is worth noting that UiO-66-$(F)_4$ has a lower working capacity (0.261 mmol g^{-1}) than that of UiO-66 although they have comparable surface areas. This is probably due to the weaker adsorbate−adsorbent interactions in UiO-66-$(F)_4$ as F-containing groups are well-known for their nonpolarity and are often used to prepare hydrophobic surface.[42] A similar conclusion can be drawn by comparing UiO-66-$(COOH)_2$ and UiO-66-$(OCH_2CH_3)_2$, both of which have similar surface areas while the working capacity of the latter (0.184 mmol g^{-1}) is only 30% of that of the former (0.620 mmol g^{-1}). The affinity strength of CO_2 toward MOFs can be quantitatively evaluated by isosteric heat of adsorption (Q_{st}) calculated according to the Clausius−Clapeyron equation.[43] The MHT-synthesized UiO-66 has a low-coverage Q_{st} of −22.2 kJ mol^{-1}, which is comparable to the literature value of −25 kJ mol^{-1} (Figure 5a and Table S2 in the Supporting Information).[38,44] It is not surprising to see that

DOI: 10.1021/acs.inorgchem.5b00435
Inorg. Chem. 2015, 54, 4862−4868

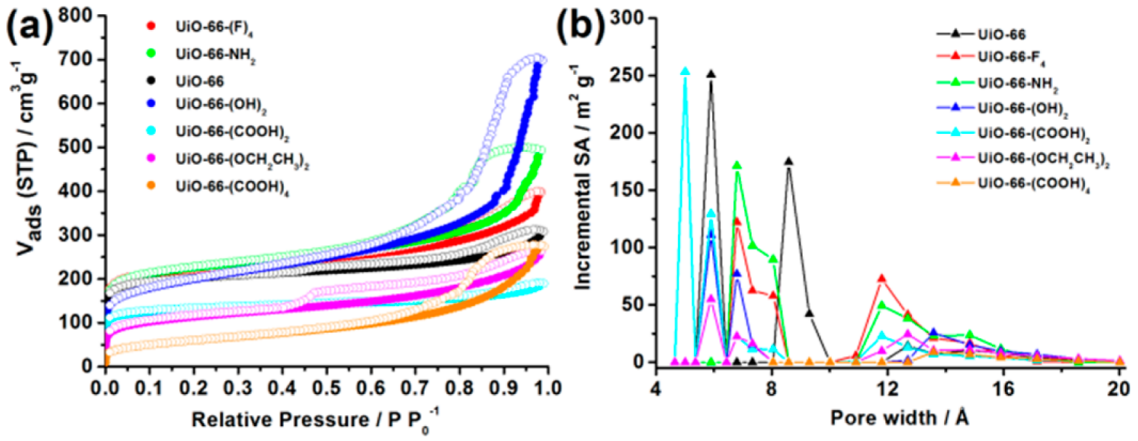

Figure 3. N_2 isotherms at 77 K (a) and pore size distribution (b) of UiO-66-type MOFs.

Table 1. Surface Area (SA), Pore Volume, and Gas Uptake of UiO-66-Type MOFs

	UiO-66 (solvothermal)	UiO-66	UiO-66-NH_2	UiO-66-$(OH)_2$	UiO-66-$(COOH)_2$	UiO-66-$(OCH_2CH_3)_2$	UiO-66-$(F)_4$	UiO-66-$(COOH)_4$
BET SA[a]	1525	769.2	833.4	705.5	494.1	405.2	833.1	212.0
Langmuir SA[a]	1757	931.2	1073.3	1011.2	608.3	574.9	1040.1	342.2
pore vol[b]	0.66	0.477	0.763	1.081	0.293	0.408	0.616	0.424
CO_2 uptake at 0.15 bar[c]								
298 K	0.37	0.339	0.585	0.651	0.620	0.184	0.261	0.209
CO_2 uptake at 1 bar[c]								
298 K	1.79	1.314	1.776	1.952	1.821	0.646	1.216	0.534
273 K	3.12	2.071	2.796	2.777	2.460	1.030	2.110	0.805
N_2 uptake at 1 bar[c]								
298 K	0.143	0.147	0.156	0.158	0.170	0.059	0.187	0.085
273 K	0.233	0.263	0.256	0.276	0.259	0.113	0.320	0.146
water uptake[d] at 273 K								
P/P_0 = 0.1	11	20	78	64	140	36	45	46
P/P_0 = 0.3	38	146	283	128	194	83	236	87
P/P_0 = 0.9	735	341	645	283	286	243	407	339

[a] $m^2\ g^{-1}$. [b] $cm^3\ g^{-1}$. [c] $mmol\ g^{-1}$. [d] $cm^3\ g^{-1}$.

UiO-66-$(COOH)_2$ has the highest low-coverage Q_{st} of −33.6 kJ mol^{-1} due to its polar groups and small pore size of ∼5 Å (Figure 3b) suitable for strong CO_2 interactions.[38] As what we have expected, UiO-66-$(F)_4$ exhibits the lowest low-coverage Q_{st} of −18.7 kJ mol^{-1} due to the nonpolar F-containing groups. The CO_2/N_2 selectivities of MHT-synthesized MOFs were calculated based on ideal adsorption solution theory (IAST), and the results are shown in Figure 5b and Table S2 in the Supporting Information.[45] Similar to the trend of Q_{st}, UiO-66-$(COOH)_2$ has the highest IAST CO_2/N_2 selectivity (35.4) at 298 K and 1 bar followed by UiO-66-$(OH)_2$ (34.2), while UiO-66-$(F)_4$ has the lowest one (16.0).

Water Sorption Isotherm Analysis. Based on the above discussion, it seems that UiO-66-$(COOH)_2$ and UiO-66-$(OH)_2$ are better candidates for postcombustion CO_2 capture due to their high working capacity and good selectivity. However, since flue gas is saturated with water vapor which will compete with CO_2 for the sorption sites leading to deteriorated CO_2 capture performance, another important factor for MOFs is low water interference, which has only been studied recently.[5,11] The various polarities of the UiO-66-type MOFs synthesized through our MHT approach motivate us to examine their water sorption behaviors (Figure 6 and Table 1). The water adsorption isotherm of solvothermally synthesized UiO-66 shows a sigmoidal shape that is identical to the reported one.[11] There is very small water uptake at $P/P_0 < 0.3$ indicating the hydrophobic nature of UiO-66. The abrupt water uptake increase at $0.3 < P/P_0 < 0.4$ represents the formation of water clusters which quickly fill the cavities of UiO-66 leading to a saturation plateau.[5] The water uptake of MHT-synthesized UiO-66 is smaller than the solvothermally synthesized one due to a lower surface area. Although the shape of the isotherm is still sigmoidal, the first bending point indicating the formation of water clusters has shifted toward a lower pressure of $P/P_0 \approx 0.2$. This is probably because of the extra defects generated during MHT that have increased the hydrophilicity of this material.[31] Due to the polar carboxylic acid groups, UiO-66-$(COOH)_2$ exhibits the steepest rise of water sorption uptake at lower pressure range leading to a type I water sorption isotherm that is identical to zeolites.[11] This normally indicates a strong water interference that is however undesirable in CO_2 capture. On the contrary, UiO-66-$(OCH_2CH_3)_2$ with nonpolar groups has a flat water isotherm with a much lower water uptake due to its hydrophobic nature. Considering its relatively high IAST CO_2/N_2 selectivity of 24.9, UiO-66-$(OCH_2CH_3)_2$ should be a better candidate for postcombustion CO_2 capture.

DOI: 10.1021/acs.inorgchem.5b00435
Inorg. Chem. 2015, 54, 4862−4868

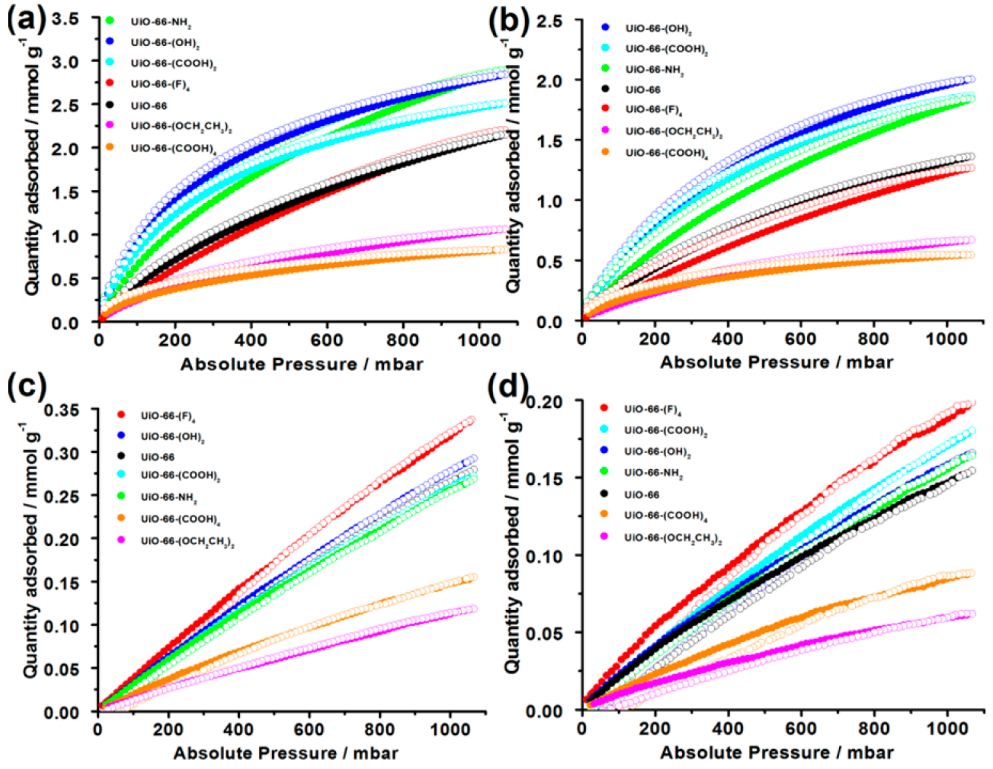

Figure 4. Gas sorption isotherms of UiO-66-type MOFs (filled, adsorption; open, desorption): (a) CO_2 at 273 K; (b) CO_2 at 298 K; (c) N_2 at 273 K; (d) N_2 at 298 K.

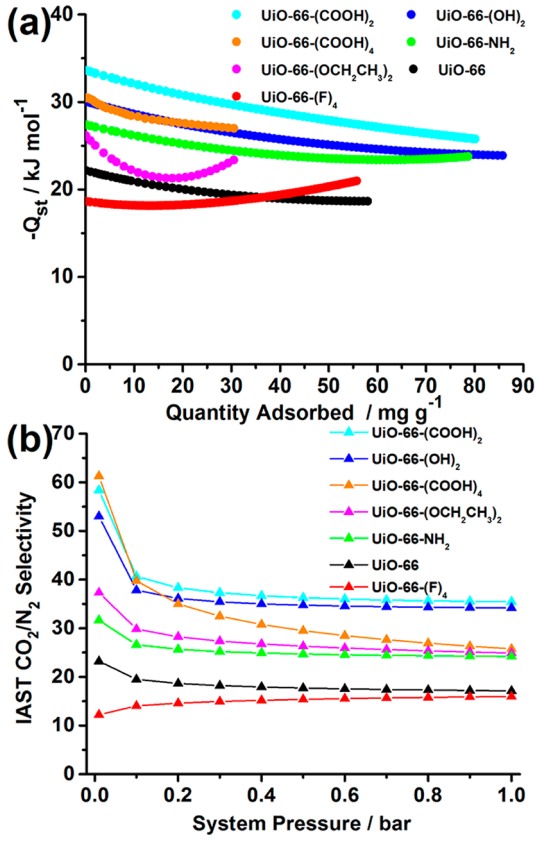

Figure 5. (a) Q_{st} of CO_2 of UiO-66-type MOFs; (b) IAST CO_2/N_2 selectivity at 298 K calculated by assuming a CO_2/N_2 binary mixture (15/85).

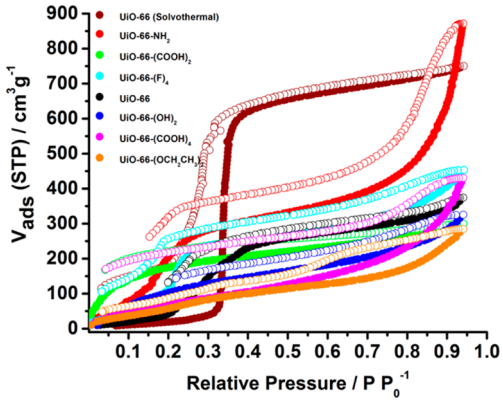

Figure 6. Water vapor sorption isotherms of UiO-66-type MOFs at 273 K (filled, adsorption; open, desorption).

CONCLUSIONS

In summary, we have successfully developed a green, mild, and scalable MHT approach for the synthesis of a series of UiO-66-type MOFs including UiO-66-$(F)_4$, UiO-66-$(OCH_2H_3)_2$, and UiO-66-$(COOH)_4$ that have not been reported previously. These MOFs are highly water-stable with extra defects serving as Lewis acid sites good for sorption and catalysis. Their performance in postcombustion CO_2 capture has been evaluated by analyzing their N_2, CO_2, and water sorption isotherms. We have found that although UiO-66-$(COOH)_2$ has a high working capacity and good selectivity, its CO_2 capture performance may be severely impaired in the presence of water. On the other hand, UiO-66-$(OCH_2CH_3)_2$ may be a better option due to its hydrophobicity that can sustain its CO_2 capture performance under real working conditions. The MHT

DOI: 10.1021/acs.inorgchem.5b00435
Inorg. Chem. 2015, 54, 4862−4868

approach reported herein can be readily applied to the existing chemical reactors, which paves a solid way toward the massive production and commercialization of promising water-stable MOFs.

■ ASSOCIATED CONTENT

Supporting Information

Experimental calculations, FE-SEM images, EDX data, and summary of the recipe and yield for MHT synthesis of UiO-66-type MOFs. The Supporting Information is available free of charge on the ACS Publications website at DOI: 10.1021/acs.inorgchem.5b00435.

■ AUTHOR INFORMATION

Corresponding Author

*E-mail: chezhao@nus.edu.sg.

Notes

The authors declare the following competing financial interest(s): A US provisional patent (No. 62/132,608) has been filed based on the presented result.

■ ACKNOWLEDGMENTS

This work is supported by National University of Singapore (NUS Start-up Funding R-279-000-369-133, CENGas R-261-508-001-646) and Singapore Ministry of Education (MOE AcRF Tier 1 R-279-000-410-112, AcRF Tier 2 R-279-000-429-112).

■ REFERENCES

(1) Furukawa, H.; Cordova, K. E.; O'Keeffe, M.; Yaghi, O. M. *Science* **2013**, *341*, 1230444.
(2) Cook, T. R.; Zheng, Y.-R.; Stang, P. J. *Chem. Rev.* **2013**, *113*, 734−777.
(3) Zhou, H. C.; Long, J. R.; Yaghi, O. M. *Chem. Rev.* **2012**, *112*, 673−674.
(4) Zhou, H.-C.; Kitagawa, S. *Chem. Soc. Rev.* **2014**, *43*, 5415−5418.
(5) Canivet, J.; Fateeva, A.; Guo, Y.; Coasne, B.; Farrusseng, D. *Chem. Soc. Rev.* **2014**, *43*, 5594−5617.
(6) Férey, G.; Mellot-Draznieks, C.; Serre, C.; Millange, F.; Dutour, J.; Surblé, S.; Margiolaki, I. *Science* **2005**, *309*, 2040−2042.
(7) Phan, A.; Doonan, C. J.; Uribe-Romo, F. J.; Knobler, C. B.; O'Keeffe, M.; Yaghi, O. M. *Acc. Chem. Res.* **2010**, *43*, 58−67.
(8) Colombo, V.; Galli, S.; Choi, H. J.; Han, G. D.; Maspero, A.; Palmisano, G.; Masciocchi, N.; Long, J. R. *Chem. Sci.* **2011**, *2*, 1311−1319.
(9) Cavka, J. H.; Jakobsen, S.; Olsbye, U.; Guillou, N.; Lamberti, C.; Bordiga, S.; Lillerud, K. P. *J. Am. Chem. Soc.* **2008**, *130*, 13850−13851.
(10) Jakobsen, S.; Gianolio, D.; Wragg, D. S.; Nilsen, M. H.; Emerich, H.; Bordiga, S.; Lamberti, C.; Olsbye, U.; Tilset, M.; Lillerud, K. P. *Phys. Rev. B* **2012**, *86*, 125429.
(11) Furukawa, H.; Gándara, F.; Zhang, Y.-B.; Jiang, J.; Queen, W. L.; Hudson, M. R.; Yaghi, O. M. *J. Am. Chem. Soc.* **2014**, *136*, 4369−4381.
(12) Bueken, B.; Reinsch, H.; Reimer, N.; Stassen, I.; Vermoortele, F.; Ameloot, R.; Stock, N.; Kirschhock, C. E. A.; De Vos, D. *Chem. Commun.* **2014**, *50*, 10055−10058.
(13) Liu, T.-F.; Feng, D.; Chen, Y.-P.; Zou, L.; Bosch, M.; Yuan, S.; Wei, Z.; Fordham, S.; Wang, K.; Zhou, H.-C. *J. Am. Chem. Soc.* **2015**, *137*, 413−419.
(14) Gutov, O. V.; Bury, W.; Gomez-Gualdron, D. A.; Krungleviciute, V.; Fairen-Jimenez, D.; Mondloch, J. E.; Sarjeant, A. A.; Al-Juaid, S. S.; Snurr, R. Q.; Hupp, J. T.; Yildirim, T.; Farha, O. K. *Chem.—Eur. J.* **2014**, *20*, 12389−12393.
(15) Beyzavi, M. H.; Klet, R. C.; Tussupbayev, S.; Borycz, J.; Vermeulen, N. A.; Cramer, C. J.; Stoddart, J. F.; Hupp, J. T.; Farha, O. K. *J. Am. Chem. Soc.* **2014**, *136*, 15861−15864.
(16) Feng, D.; Wang, K.; Su, J.; Liu, T.-F.; Park, J.; Wei, Z.; Bosch, M.; Yakovenko, A.; Zou, X.; Zhou, H.-C. *Angew. Chem., Int. Ed.* **2015**, *54*, 149−154.
(17) Kalidindi, S. B.; Nayak, S.; Briggs, M. E.; Jansat, S.; Katsoulidis, A. P.; Miller, G. J.; Warren, J. E.; Antypov, D.; Corà, F.; Slater, B.; Prestly, M. R.; Martí-Gastaldo, C.; Rosseinsky, M. J. *Angew. Chem., Int. Ed.* **2015**, *54*, 221−226.
(18) Nugent, P.; Belmabkhout, Y.; Burd, S. D.; Cairns, A. J.; Luebke, R.; Forrest, K.; Pham, T.; Ma, S. Q.; Space, B.; Wojtas, L.; Eddaoudi, M.; Zaworotko, M. J. *Nature* **2013**, *495*, 80−84.
(19) Stock, N.; Biswas, S. *Chem. Rev.* **2012**, *112*, 933−969.
(20) Friščić, T.; Halasz, I.; Beldon, P. J.; Belenguer, A. M.; Adams, F.; Kimber, S. A.; Honkimäki, V.; Dinnebier, R. E. *Nat. Chem.* **2013**, *5*, 66−73.
(21) Faustini, M.; Kim, J.; Jeong, G.-Y.; Kim, J. Y.; Moon, H. R.; Ahn, W.-S.; Kim, D.-P. *J. Am. Chem. Soc.* **2013**, *135*, 14619−14626.
(22) Rubio-Martinez, M.; Batten, M. P.; Polyzos, A.; Carey, K.-C.; Mardel, J. I.; Lim, K.-S.; Hill, M. R. *Sci. Rep.* **2014**, *4*, 5443.
(23) Yang, Q.; Vaesen, S.; Ragon, F.; Wiersum, A. D.; Wu, D.; Lago, A.; Devic, T.; Martineau, C.; Taulelle, F.; Llewellyn, P. L. *Angew. Chem., Int. Ed.* **2013**, *125*, 10506−10510.
(24) Hu, Z.; Khurana, M.; Seah, Y. H.; Zhang, M.; Guo, Z.; Zhao, D. *Chem. Eng. Sci.* **2015**, *124*, 61−69.
(25) Zhao, Q.; Yuan, W.; Liang, J.; Li, J. *Int. J. Hydrogen Energy* **2013**, *38*, 13104−13109.
(26) Katz, M. J.; Brown, Z. J.; Colón, Y. J.; Siu, P. W.; Scheidt, K. A.; Snurr, R. Q.; Hupp, J. T.; Farha, O. K. *Chem. Commun.* **2013**, *49*, 9449−9451.
(27) Vermoortele, F.; Bueken, B.; Le Bars, G.; Van de Voorde, B.; Vandichel, M.; Houthoofd, K.; Vimont, A.; Daturi, M.; Waroquier, M.; Van Speybroeck, V. *J. Am. Chem. Soc.* **2013**, *135*, 11465−11468.
(28) Ragon, F.; Horcajada, P.; Chevreau, H.; Hwang, Y. K.; Lee, U.-H.; Miller, S. R.; Devic, T.; Chang, J.-S.; Serre, C. *Inorg. Chem.* **2014**, *53*, 2491−2500.
(29) Ren, J.; Langmi, H. W.; North, B. C.; Mathe, M.; Bessarabov, D. *Int. J. Hydrogen Energy* **2014**, *39*, 890−895.
(30) Wu, H.; Chua, Y. S.; Krungleviciute, V.; Tyagi, M.; Chen, P.; Yildirim, T.; Zhou, W. *J. Am. Chem. Soc.* **2013**, *135*, 10525−10532.
(31) Øien, S.; Wragg, D.; Reinsch, H.; Svelle, S.; Bordiga, S.; Lamberti, C.; Lillerud, K. P. *Cryst. Growth Des.* **2014**, *14*, 5370−5372.
(32) Cliffe, M. J.; Wan, W.; Zou, X.; Chater, P. A.; Kleppe, A. K.; Tucker, M. G.; Wilhelm, H.; Funnell, N. P.; Coudert, F.-X.; Goodwin, A. L. *Nat. Commun.* **2014**, *5*, 4176.
(33) Fang, Z.; Dürholt, J. P.; Kauer, M.; Zhang, W.; Lochenie, C.; Jee, B.; Albada, B.; Metzler-Nolte, N.; Pöppl, A.; Weber, B.; Muhler, M.; Wang, Y.; Schmid, R.; Fischer, R. A. *J. Am. Chem. Soc.* **2014**, *136*, 9627−9636.
(34) Britt, D.; Furukawa, H.; Wang, B.; Glover, T. G.; Yaghi, O. M. *Proc. Natl. Acad. Sci. U.S.A.* **2009**, *106*, 20637−20640.
(35) Barin, G.; Krungleviciute, V.; Gutov, O.; Hupp, J. T.; Yildirim, T.; Farha, O. K. *Inorg. Chem.* **2014**, *53*, 6914−6919.
(36) Hwang, Y. K.; Hong, D.-Y.; Chang, J.-S.; Jhung, S. H.; Seo, Y.-K.; Kim, J.; Vimont, A.; Daturi, M.; Serre, C.; Férey, G. *Angew. Chem., Int. Ed.* **2008**, *47*, 4144−4148.
(37) Kozachuk, O.; Luz, I.; Llabrés i Xamena, F. X.; Noei, H.; Kauer, M.; Albada, H. B.; Bloch, E. D.; Marler, B.; Wang, Y.; Muhler, M.; Fischer, R. A. *Angew. Chem., Int. Ed.* **2014**, *53*, 7058−7062.
(38) Hu, Z.; Zhang, K.; Zhang, M.; Guo, Z.; Jiang, J.; Zhao, D. *ChemSusChem* **2014**, *7*, 2791−2795.
(39) Myers, S. S.; Zanobetti, A.; Kloog, I.; Huybers, P.; Leakey, A. D.; Bloom, A. J.; Carlisle, E.; Dietterich, L. H.; Fitzgerald, G.; Hasegawa, T. *Nature* **2014**, *510*, 139−142.
(40) Sumida, K.; Rogow, D. L.; Mason, J. A.; McDonald, T. M.; Bloch, E. D.; Herm, Z. R.; Bae, T. H.; Long, J. R. *Chem. Rev.* **2012**, *112*, 724−781.
(41) Bae, T. H.; Hudson, M. R.; Mason, J. A.; Queen, W. L.; Dutton, J. J.; Sumida, K.; Micklash, K. J.; Kaye, S. S.; Brown, C. M.; Long, J. R. *Energy Environ. Sci.* **2013**, *6*, 128−138.

DOI: 10.1021/acs.inorgchem.5b00435
Inorg. Chem. 2015, 54, 4862−4868

(42) Dalvi, V. H.; Rossky, P. J. *Proc. Natl. Acad. Sci. U.S.A.* **2010**, *107*, 13603−13607.
(43) Rowsell, J. L. C.; Yaghi, O. M. *J. Am. Chem. Soc.* **2006**, *128*, 1304−1315.
(44) Cmarik, G. E.; Kim, M.; Cohen, S. M.; Walton, K. S. *Langmuir* **2012**, *28*, 15606−15613.
(45) Myers, A. L.; Prausnitz, J. M. *AIChE J.* **1965**, *11*, 121−127.

DOI: 10.1021/acs.inorgchem.5b00435
Inorg. Chem. 2015, 54, 4862−4868